Implementation of Integer Factor based Space Vector PWM through Digital Approach for Grid Connected Multilevel Inverters

A. Suresh Kumar*‡ (iD), K. Sri Gowri** (iD), S. Nagaraja Rao*** (iD), B.M. Manjunatha* (iD),

N. Mallikarjuna**** (iD), Durga Prasad Garapati***** (iD)

* Department of EEE, Rajeev Gandhi Memorial College of Engineering and Technology, Nandyal, Andhra Pradesh, India.

**Department of EEE, G Pulla Reddy Engineering College, Kurnool, Andhra Pradesh, India.

*** Department of EE, M.S. Ramaiah University of Applied Sciences, Bangalore, Karnataka, India.

**** Department of EEE, The National Institute Engineering, Mysore, India.

***** Department of EEE, Shri Vishnu Engineering College for Women, Andhra Pradesh, India.

(surianisetty@gmail.com, gowrivasu.3@gmail.com, nagarajarao.ee.et@msruas.ac.in, manjumtech003@gmail.com, j.malli243@gmail.com, durgaprasad_garapati@svecw.edu.in)

‡ Corresponding Author; A. Suresh Kumar, Department of EEE, RGMCET, Nandyal, Andhra Pradesh, India, Tel: +919440972229, e-mail: surianisetty@gmail.com

Abstract- Space vector pulse width modulation control for grid connected multilevel inverters are very popular. However, it gets exceedingly tough with the increase in the number of output voltage levels. The total number of possible switching states will increase with the output voltage level of the inverter. Due to increase in the number of switching states, the sub triangles in the various sectors of the hexagon will also increase, that result in increased complexity and storage requirements for implementation using conventional space vector methods. The objective of the paper is to simplify and generalize the space vector algorithm for an n-level inverter. The proposed algorithm uses integer factor approach to find the exact location of the reference vector, synthesize switching times and generate the nearby switching states. It is a generalized algorithm applicable to any sequence and can be applied to any level judiciously. In this article description of the algorithm is given for a three–level inverter and validated by implementing experimentally using dspace control desk. The PWM signals generated by three level Space Vector algorithm with conventional switching sequence of 0127 is used to control an open end winding induction motor fed with two two-level inverters. The performance factor of motor voltage and line current THD at different modulation index is measured and compared with simulation result.

Keywords Integer Factor Approach; Space Vector Modulation; Multilevel Inverters; Inverters; SVPWM; Optimum Switching Sequence.

1. Introduction

Recently MLI inverters are widely used in various grid connected systems due to the several advantages of reduced energy consumption, better system efficiency, less dv/dt and less total harmonic distortion (THD) of the output voltage [1]-[6]. So far different Pulse Width Modulation (PWM) control methods are presented. Among the existing control methods sine PWM (SPWM) and space vector modulation (SVM) are the better methods to control the MLIs [7]-[9]. Among these, SVM method is widely preferred than carrier comparison method due to complete digital implementation. Furthermore, having advantages of high D.C bus voltage, improved power quality with less THD and common mode voltage [9]. But as the number of levels increases the conventional SVM approach become significantly complex.

The various SVM algorithms have been developed in the past to control of MLIs. The authors in [10], [11] proposed SVM concept based on standard two-level concept. This involves huge complex mathematical calculations. To extend this method to the higher level of inverter is more complex due increased reference vector identification stages. In [12], [13] proposed SVM based on carrier based, which is not involved direct digital implementation. This type of approach required huge memory in the controller to store more number of carrier signals as levels increases in the inverter and also more delay in the execution time. In [14] the reference vector is shifted to a two level hexagon with its pivot vector exactly at the midpoint of a-phase for the decomposition process. In

this method reference vector related to higher level is decomposed into to two level hexagons through several stages by identifying midpoint of the vector. But, as levels increases in the inverter these decomposition stages are increased. So that implementation of this method to the higher levels is complex. In [15] a Cartesian coordinate's based approach is proposed using two factors k1 and k2. This approach is similar to the standard two level SV approach, but can't exclude the need of lookup table. In [16] a scheme using fractal based approach is proposed, but it requires indication of triangle to generate switching states. It is difficult and become complex as level increases in the inverter. In [17] online computation of switching pulses is done through l-factor approach where in generalized equations are given for each switch to derive modulating signal after which carrier comparison approach is taken up to synthesize switching pulses. To utilize the freedom of space vector approach and generate different discontinuous modulating signals, the generalized equations need to be changed which is a tedious process and not suitable for digital implementation. In [18] with a similar approach freedom of choosing the zero state duration is investigated and also the nearest three switching states including redundant states are synthesized with generalized equation. But generalization of active sate is not addressed clearly. The authors in [19]-[20] proposed SVPWM based an offset vector. In this the position of the offset vector need to identify to find subsectors. But, it involves more mathematical calculations to identify offset vector location. In [21] a simple reverse mapping based SVM is suggested for n-level MLI, but not addressed selection of redundant vectors states. In [22] decomposition-based SVM is analyzed, however the extension of this method to higher levels necessitates the identification of more decomposition stages by locating the intermediate vector. As the number of levels increases, this becomes more challenging.

By Understanding the credibility's and problems with different implementation algorithms employed by the researchers in the past, a new SVM algorithm for MLI is proposed in this paper and it can be easily extended to advanced DPWM methods like [23-24]. This method is developed based on Integer factor approach (IFA) by focussing on feasible to digital implementation. So, it can be easily developed on low cost controllers with minimum execution time. Also, complex mathematical calculations are not there in the algorithm and the computational efforts do not increase for higher level inverter. Also the inherent advantage of this approach is, it can be used to generate different discontinuous PWM (DPWM) pulses.

2. Proposed SVPWM Using IFA

This approach will encompass to determine i) sector and sub triangle location of the reference vector ii) Switching times iii) Switching states (including the redundant states). The step by step process of proposed SVM implementation using IFA is shown in Fig.1 with help of the block diagram. The state space diagram with reliable switching states and sub triangles for three-level inverter is depicted in Fig.2 in the form of hexagon with six symmetrical sectors and four sub

triangles in each sector selected by 'p and q' where "p" is the sector number and "q" is sub triangle sector number. There are two different types of sub triangles: type-1 and type-2. Type-1 triangles have their apex facing up and type-2 triangles have it facing down. Out of the four sub triangles in sector 1, type-1 consists of three sub triangles i.e., 10, 11, 13 and type-2 consists of sub triangle 12.

2.1. 3-Phase To 2-Phase Conversion and Sector Identification

The reference voltage vector, is synthesized from the instantaneous three phase sinusoidal voltages as follows:

$$V_a = V_m \sin \omega t \qquad (1)$$

$$V_b = V_m \sin\left(\omega t - \frac{2\pi}{3}\right) \qquad (2)$$

$$V_c = V_m \sin\left(\omega t - \frac{4\pi}{3}\right) \qquad (3)$$

Clarke's transformation is used to convert 3-Φ voltages to 2-Φ voltages using, (4) and from the 2-Φ voltages the magnitude and position of V_{ref} is synthesized using equations (5) - (6).

$$\begin{bmatrix} V_q \\ V_d \end{bmatrix} = \frac{2}{3}\begin{bmatrix} 1 & \dfrac{-1}{2} & \dfrac{-1}{2} \\ 0 & \dfrac{\sqrt{3}}{2} & \dfrac{-\sqrt{3}}{2} \end{bmatrix} \qquad (4)$$

$$V_{ref} = \sqrt{V_d^2 + V_q^2} \qquad (5)$$

$$\alpha = \tan^{-1}\left(\frac{V_d}{V_q}\right) \qquad (6)$$

The sector, k in which V_{ref} lies is identified from equation (7).

$$k = \text{int}\left(\frac{\alpha}{60^0}\right) + 1 \qquad (7)$$

Once the location of V_{ref} is identified in terms a sector, sub triangle need to be identify for which integer factors need to be synthesized at every sampling instant.

2.2. Determination Integer Factors and Sub Triangle

Sub triangle in which V_{ref} is located is made through the integer factors of the corresponding sub triangle. For instance, V_{ref} at a given switching instant is located as shown in Fig.3.
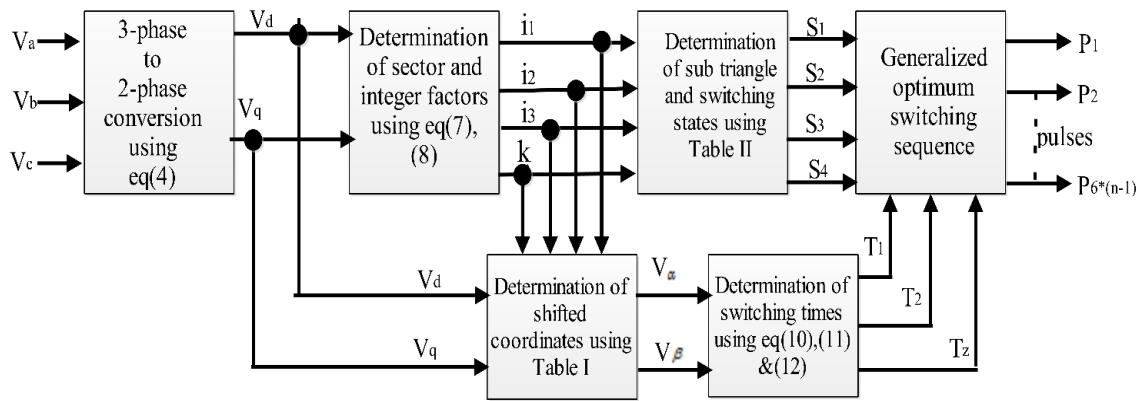
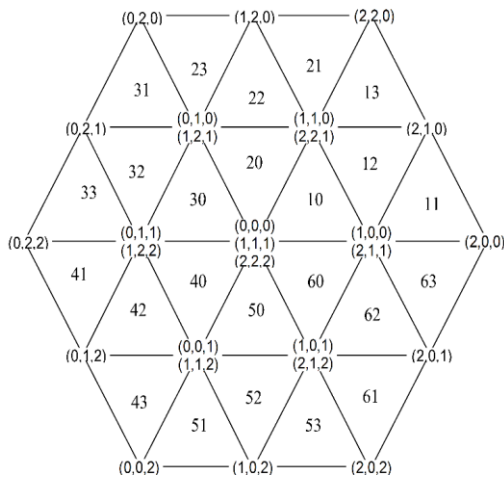**Fig.1** Block diagram of proposed SVM implementation using integer approach

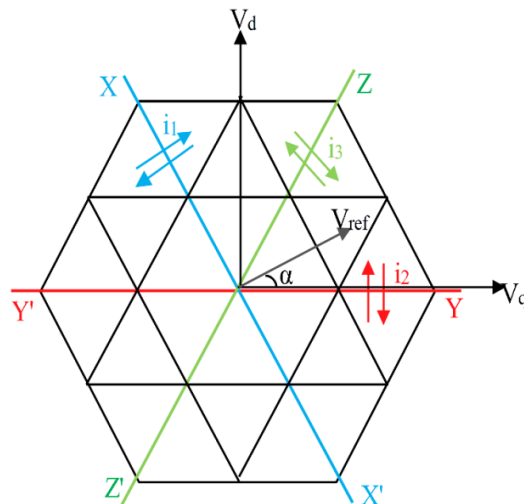**Fig.2** State space diagram with switching states and sub triangles

Fig.3. Movement of X-X', Y-Y' and Z-Z' axes

The space vector plane is made up of three lines: X-X', Y-Y', and Z-Z'. Each of these lines can move back and forth with respect to their reference axes. As illustrated in Fig.3, the reference axes are inclined at an angle of 120^0, 0^0, 60^0 with respect to the q-axis. The reference axis may be either positive or negative real values at a given modulation index (MI), depending on the reference vector (V_{ref}) instantaneous position. MI is defined for a MLI in (8).

$$MI = \frac{3}{2}\left(\frac{V_{ref}}{V_{dc}/(n-1)}\right) \qquad (8)$$

The tip of the reference vector is in a sub triangle, which can be found by sliding the three line segments so that the tip of Vref is inside the sub triangle. There could be positive or negative values for the three lines depending on how far the axes move off of their reference axes as they move around their tips, as shown in Fig. 4. Using the proposed approach, it is sufficient to know the shortened values of shifted axes from their equivalent reference axes, which are identified by the integer factors of i_1, i_2, i_3. For a given modulation index the integer factors are derived using equations (9), (10) and (11) based on d-axis and q-axis components of $V_{ref.}$

$$i_1 = \text{int}\left(V_d + \frac{V_q}{\sqrt{3}}\right) \qquad (9)$$

$$i_2 = \text{int}\left(\frac{V_q}{\sqrt{3}}\right) \qquad (10)$$

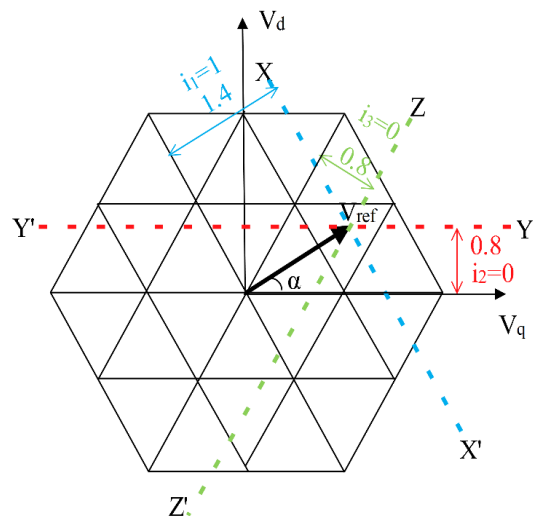$$i_3 = \text{int}\left(V_d - \frac{V_q}{\sqrt{3}}\right) \qquad (11)$$

Fig.4. Determination of IF's at a given instant

Using the integer factors (IF) sub triangle surrounds by the tip of V_{ref} will be identified. The sub triangles with a unique combination of i_1, i_2, i_3 are shown in Fig.5 for wide range of MI.
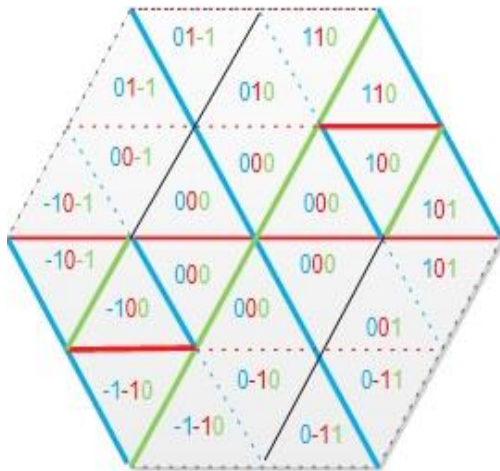

Fig.5. Sub triangles with a unique mixture of IF

2.3. Determination of the switching state times

After recognising the sub triangle in which the reference vector is situated, the switching times are to be calculated using IF's. This involves shifting the origin of the V_{ref} from three level hexagon to new origin. This new vector is referred as V^*_{ref} i.e., shifted reference vector. One of the sub triangle's three vertices will serve as the new origin of V^*_{ref}. To illustrate this process consider the transition of V_{ref} between sub triangles 11 and 13, followed by sub triangle 12. The sub triangle 11 is a type-1 sub triangle, the sub triangle 12 is a type-2 sub triangle, and the sub triangle 13 is again type-1 sub triangle, as illustrated in Fig.6. Let suppose the V_{ref} is in sub triangle-11. For this the new origin will be the left vertex seeing in the direction of V_{ref}.

Similarly for type -2 sub triangle it is the right vertex seeing in the direction of V_{ref}. After finding the origin of the V^*_{ref}, the magnitude of V^*_{ref} is determined by subtracting V_o vector from V_{ref}. Here V_o is the vector joining the centre of the three level hexagons to origin of V^*_{ref}. Therefore, the magnitude of V^*_{ref} at any instant is determined based IF's of particular sub triangle, because the origin of V^*_{ref} is depends on type of sub tringle. Than d-q axes components of the V^*_{ref} are designated as, V_α, V_β respectively. Table 1 shows generalized expressions that can be used to figure out the components for all sectors.

The factor $(-1)^{i_1+i_2+i_3}$ distinguishes the type of sub triangle, based on which the switching times of the needed states are implemented for optimal inverter performance. For instance, the switching time equations for V^*_{ref} in sub triangle -11 are similar to that of the switching time equations for V_{ref} in sub triangle-10. Similarly, if V^*_{ref} lies in sub triangle-12 the active state switching time equations are same as for V_{ref} in sub triangle-40. These are deduced by applying the volt-second balance principle and are shown in Table 2. Here T_1 and T_2 are the active state times and T_z is the zero state switching time synthesized from (12).
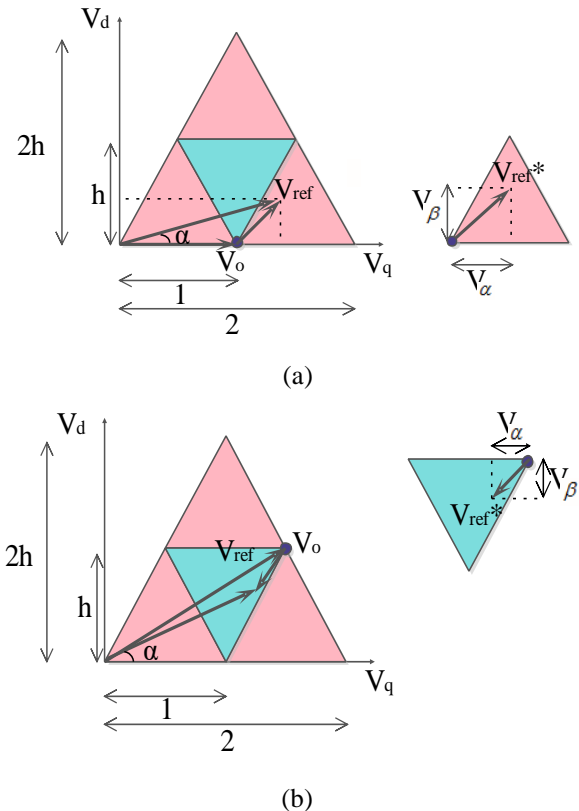
$$T_z = T_s - T_1 - T_2 \qquad (12)$$

(a)

(b)

Fig.6. Transit of V_{ref} in Sector-1 (a) V^*_{ref} coordinates in type-1 sub triangle 11 (b) V^*_{ref} coordinates in type-2 sub triangle12

2.4. Switching States Generation

The major difficulty with the SVM is locating the sub triangle in which the tip of the reference vector is present. In the preceding sections it is resolved with ease with the proposed concept of integer factors. With this the magnitude and position of the vector to be resolved at a given switching instant and the switching state times of each state are determined simply in the same way as in the case of a conventional two level inverter. But the switching states also changes with sub triangle which are yet to be recognized. Also in MLI few redundant states are available. Utilizing these switching states may reduce the number switch transitions, thereby reducing the switching losses of the inverter [12]. One way of resolving the issue is using lookup table which needs huge storage and reduce processing speed during real time implementation. With the proposed algorithm IF are used to synthesize the four optimum switching states. Fig.7 shows the position of four switching states S_1, S_2, S_3, S_4 of type-1 and type-2 sub triangles with their integer values i_1, i_2, i_3. The four switching states are synthesized through generalized equations using the integer values of the corresponding sub triangle. The generalized expressions for sector-1 are tabulated in Table 3. Here 'I' is the matrix containing integer factors as its elements.

Table 1. Shifted reference vector components: V_α and V_β

K	Angle(α)	V_α	V_β
1	$0^o \le \alpha \le 60^o$	$(-1)^{i_1+i_2+i_3}\left(V_q+0.5i_2-i_1-0.25\right)+0.25$	$(-1)^{i_1+i_2+i_3}\left(V_q-(i_2*h)-0.5h\right)+0.5h$
2	$60^o \le \alpha \le 90^o$	$(-1)^{i_1+i_2+i_3}\left(V_q+0.5i_2-i_1-0.25\right)+0.25$	$(-1)^{i_1+i_2+i_3}\left(V_q-(i_2*h)-0.5h\right)+0.5h$
	$90^o \le \alpha \le 120^o$	$(-1)^{i_1+i_2+i_3}\left(V_q+0.5i_2-i_1+0.75\right)-0.75$	$(-1)^{i_1+i_2+i_3}\left(V_q-(i_2*h)-0.5h\right)+0.5h$
3	$120^o \le \alpha \le 180^o$	$(-1)^{i_1+i_2+i_3}\left(V_q+0.5i_2-i_1+0.75\right)-0.75$	$(-1)^{i_1+i_2+i_3}\left(V_q-(i_2*h)-0.5h\right)+0.5h$
4	$180^o \le \alpha \le 240^o$	$(-1)^{i_1+i_2+i_3}\left(V_q+0.5i_2-i_1+0.25\right)-0.25$	$(-1)^{i_1+i_2+i_3}\left(V_q-(i_2*h)+0.5h\right)-0.5h$
5	$240^o \le \alpha \le 270^o$	$(-1)^{i_1+i_2+i_3}\left(V_q+0.5i_2-i_1+0.25\right)-0.25$	$(-1)^{i_1+i_2+i_3}\left(V_q-(i_2*h)+0.5h\right)-0.5h$
	$270^o \le \alpha \le 300^o$	$(-1)^{i_1+i_2+i_3}\left(V_q+0.5i_2-i_1-0.75\right)+0.75$	$(-1)^{i_1+i_2+i_3}\left(V_q-(i_2*h)+0.5h\right)-0.5h$
6	$300^o \le \alpha \le 360^o$	$(-1)^{i_1+i_2+i_3}\left(V_q+0.5i_2-i_1-0.75\right)+0.75$	$(-1)^{i_1+i_2+i_3}\left(V_q-(i_2*h)+0.5h\right)-0.5h$

Table 2. Switching times of each sector

Sector	T_1	T_2
1	$T_s\left[V_\alpha-\dfrac{V_\beta}{\sqrt{3}}\right]$	$T_s\left[\dfrac{V_\beta}{h}\right]$
2	$T_s\left[-V_\alpha+\dfrac{V_\beta}{\sqrt{3}}\right]$	$T_s\left[V_\alpha+\dfrac{V_\beta}{\sqrt{3}}\right]$
3	$T_s\left[\dfrac{V_\beta}{h}\right]$	$T_s\left[-V_\alpha-\dfrac{V_\beta}{\sqrt{3}}\right]$
4	$-T_s\left[V_\alpha-\dfrac{V_\beta}{\sqrt{3}}\right]$	$-T_s\left[\dfrac{V_\beta}{h}\right]$
5	$-T_s\left[-V_\alpha+\dfrac{V_\beta}{\sqrt{3}}\right]$	$-T_s\left[V_\alpha+\dfrac{V_\beta}{\sqrt{3}}\right]$
6	$-T_s\left[\dfrac{V_\beta}{h}\right]$	$-T_s\left[-V_\alpha-\dfrac{V_\beta}{\sqrt{3}}\right]$

Sector	Switching states	Type of triangle	
		Type-1	Type-2
1	S_1	I-[0 0 i_3]	I-[0 0 i_3]
	S_2	S1+[1 0 0]	S1+[0 1 0]
	S_3	S2+[0 1 0]	S2+[1 0 0]
	S_4	S3+[0 0 1]	S3+[0 0 1]
2	S_1	I-[0 0 i_3]	I-[0 0 i_3]
	S_2	S1+[0 1 0]	S1+[1 0 0]
	S_3	S2+[1 0 0]	S2+[0 1 0]
	S_4	S3+[0 0 1]	S3+[0 0 1]
3	S_1	I-[i_1 i_1 i_1+i_3]	I-[i_1 i_3+i_2 i_1+i_3]
	S_2	S1+[0 1 0]	S1+[0 0 1]
	S_3	S2+[0 0 1]	S2+[0 1 0]
	S_4	S3+[1 0 0]	S3+[1 0 0]
4	S_1	I-[$i_1 i_1$ i_1+i_3]	I-[i_1 i_3-i_2 i_1+i_3]
	S_2	S1+[0 0 1]	S1+[0 1 0]
	S_3	S2+[0 1 0]	S2+[0 0 1]
	S_4	S3+[1 0 0]	S3+[1 0 0]
5	S_1	I-[$i_2 i_2$ i_2+i_3]	I-[$i_1 i_2$ i_2+i_3]
	S_2	S1+[0 0 1]	S1+[1 0 0]
	S_3	S2+[1 0 0]	S2+[0 0 1]
	S_4	S3+[0 1 0]	S3+[0 1 0]
6	S_1	I-[$i_2 i_2$ i_1]	I-[-(i_3-i_1) i_2 i_3+i_2]
	S_2	S1+[1 0 0]	S1+[0 0 1]
	S_3	S2+[0 0 1]	S2+[1 0 0]
	S_4	S3+[0 1 0]	S3+[0 1 0]

3. Simulation Results

The simulation of proposed SVPWM algorithm based on integer factor approach is done using MATLAB/Simulink. The performance of this algorithm is analyzed by applying on volts/Hz controlled open-end winding induction motor at no load without filters. As shown in Fig.8, two two-level inverters are used to feed both sides of the stator windings of the induction motor to obtain three level output.
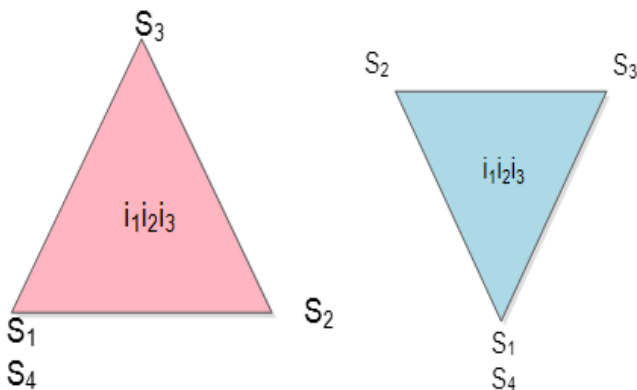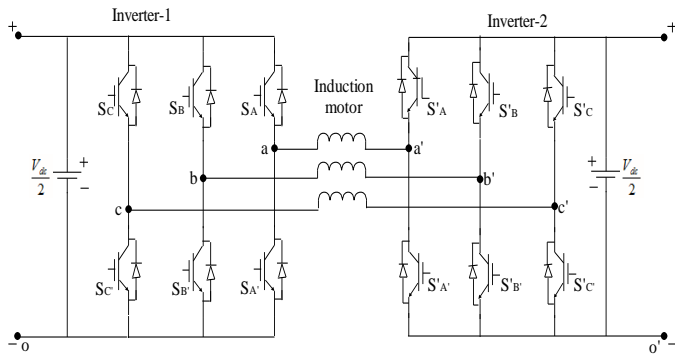

Fig.7. Switching states S_1, S_2, S_3, S_4 and their location for type-1 and type-2 sub triangles

Table 3. Optimal switching states of all sectors

Fig.8. Realization of three-level output from two, two-level inverters for an open-end winding induction motor

The three level SV pulses generated by the proposed algorithm are further bifurcated and applied to two two-level inverters. Therefore, realization of three-level output is possible through two, two-level inverters presented in [11]. The three voltage levels are attained across each phase of the three stator windings depending on the switching states of the two inverters given in Table 4.

Table 4. Voltage levels across open end winding of a phase

Level	Inverter-1	Inverter-II	Voltage across phase 'a'
0	OFF	ON	$-V_{dc}/2$
1	OFF	OFF	0
2	ON	OFF	$+V_{dc}/2$

The simulation is performed by taking switching frequency of 2kHz and the input dc voltage of 240V. The performance factor in terms of motor voltage, motor current THD at no load is studied at different MI with conventional switching sequences of 0127.
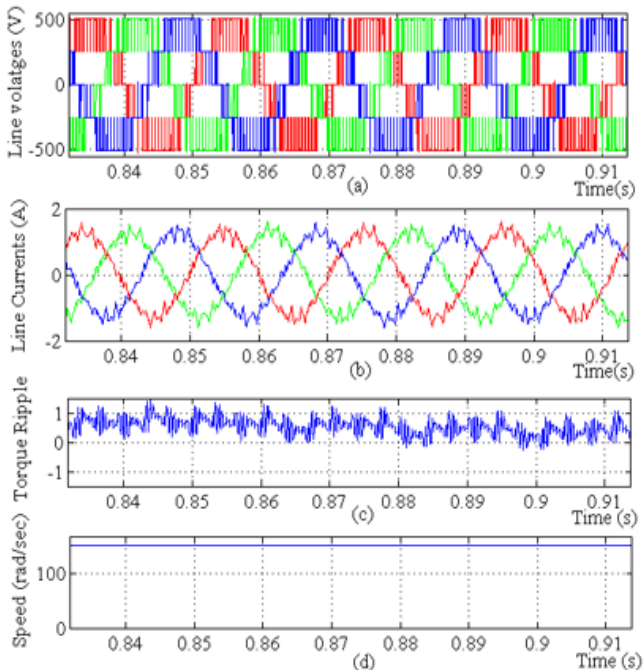

Fig.9: Simulation results at MI of 0.86; a) Three phase Line-voltages b) Three phase Line-currents c) Motor torque ripple and d) Speed

The simulation results of three phase line-voltages, line-

currents, motor torque ripple and speed are presented in Fig.9 at MI of 0.86. The performance of inverter is studied in terms of voltage and current THD at various MI and results are presented along with waveforms in Fig.10 to Fig.13.
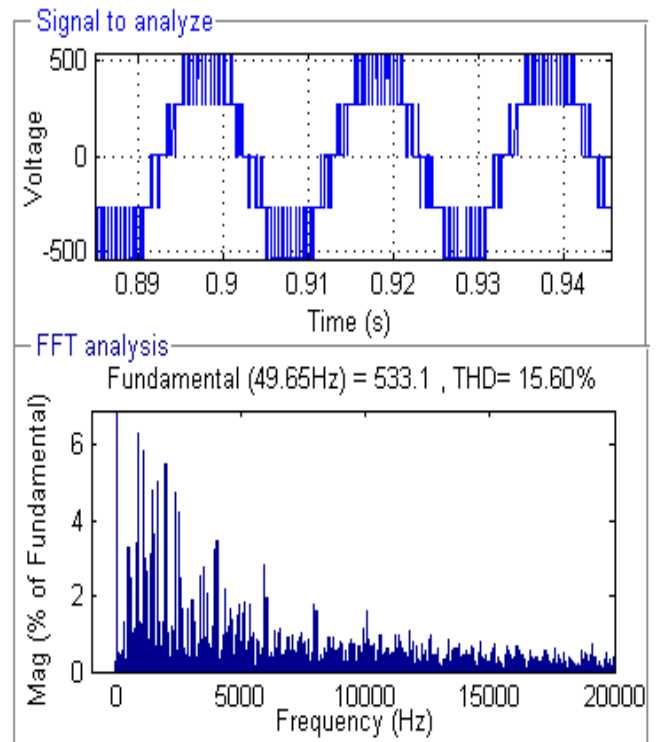
(a)
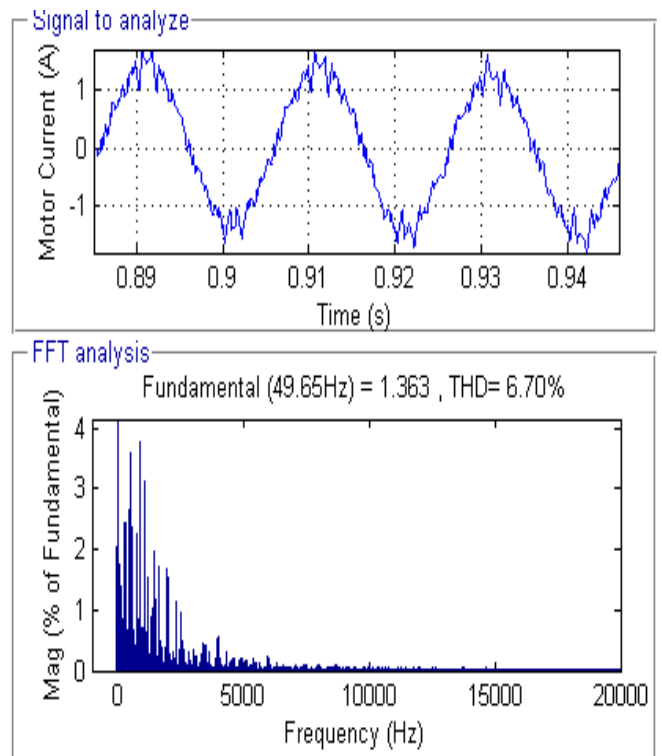
(b)

Fig.10. Output waveforms along with THD at modulation index of 0.86. a) Motor voltage b) Motor No-load current
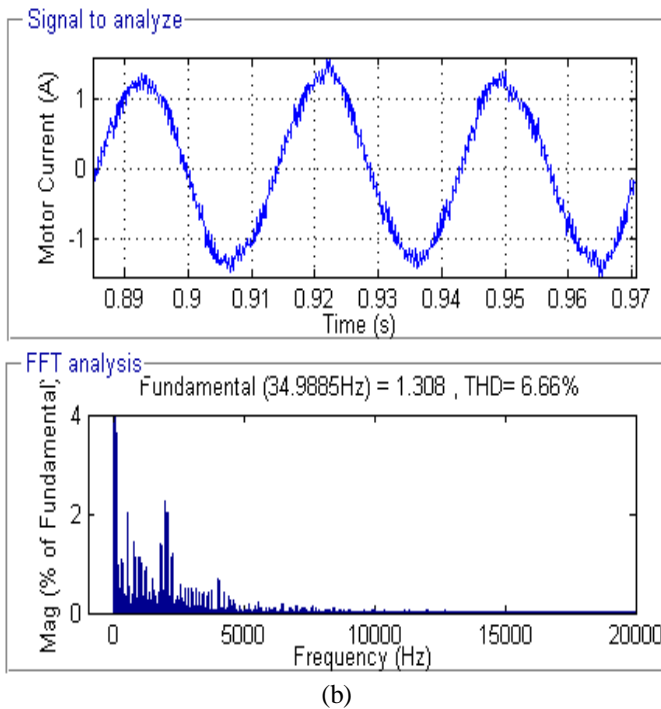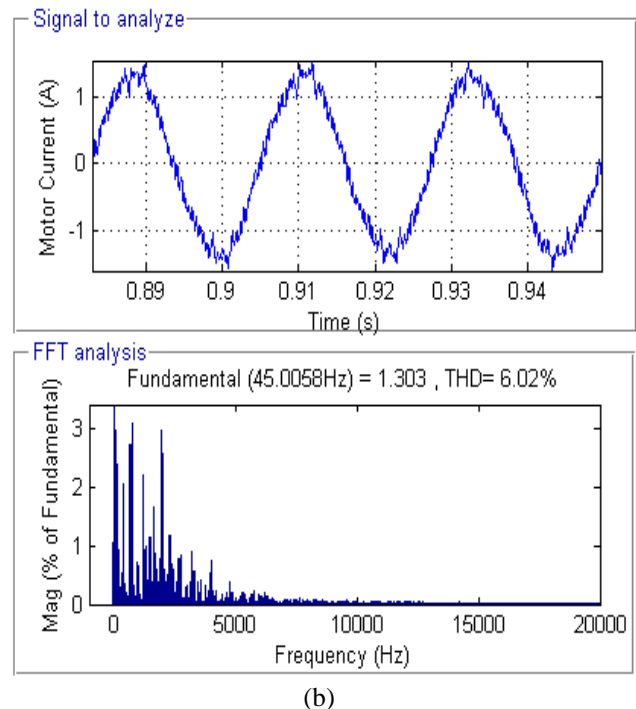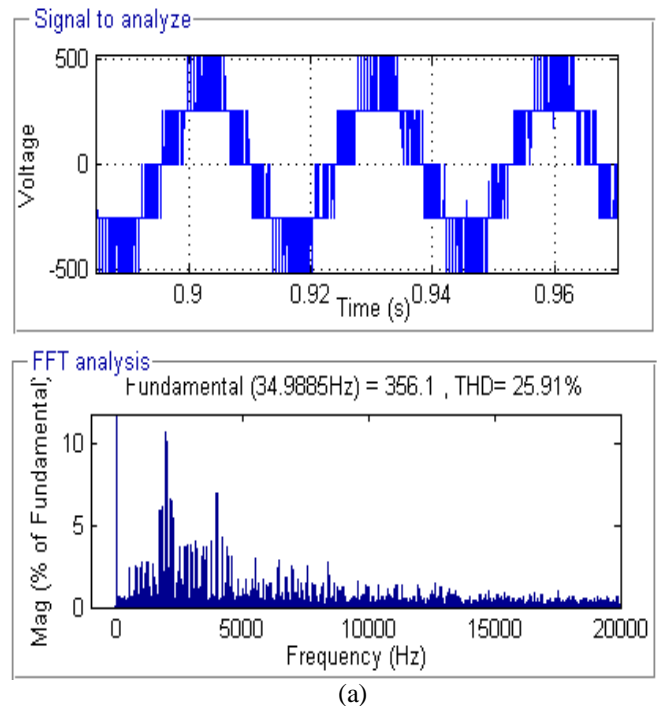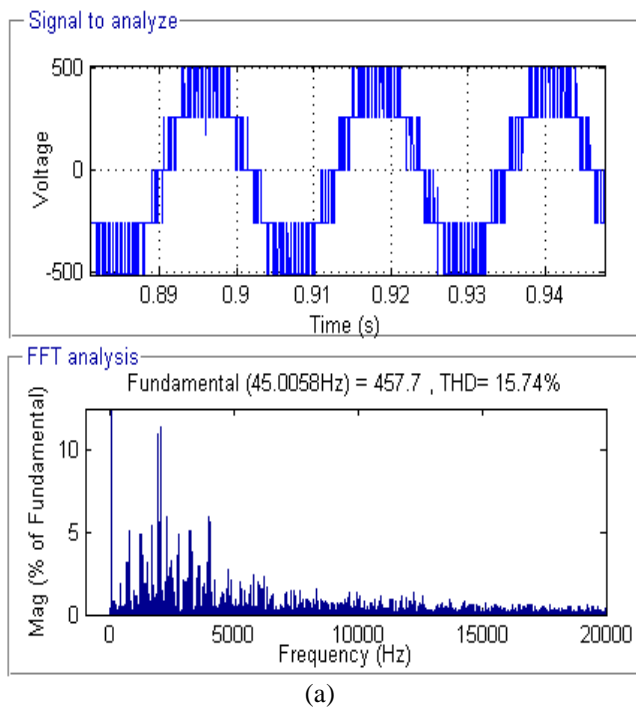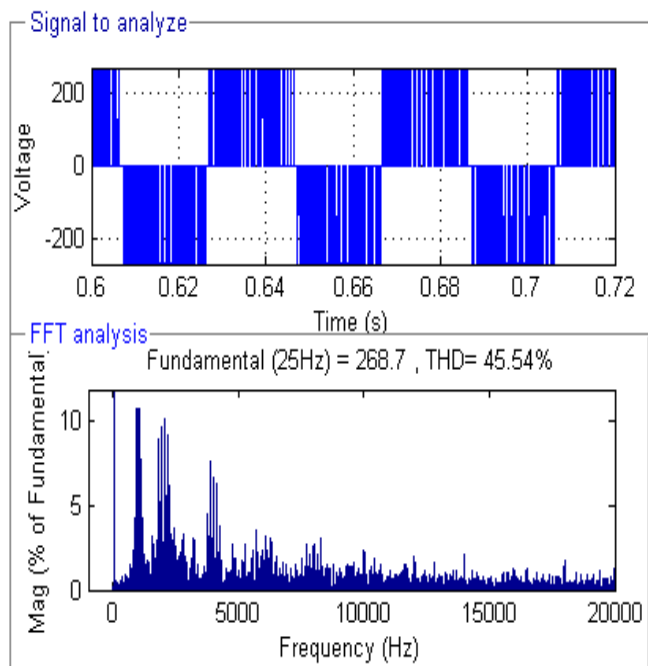
(a)

(b)

Fig.11. Output waveforms along with THD at modulation index of 0.77. a) Motor voltage b) Motor No-load current
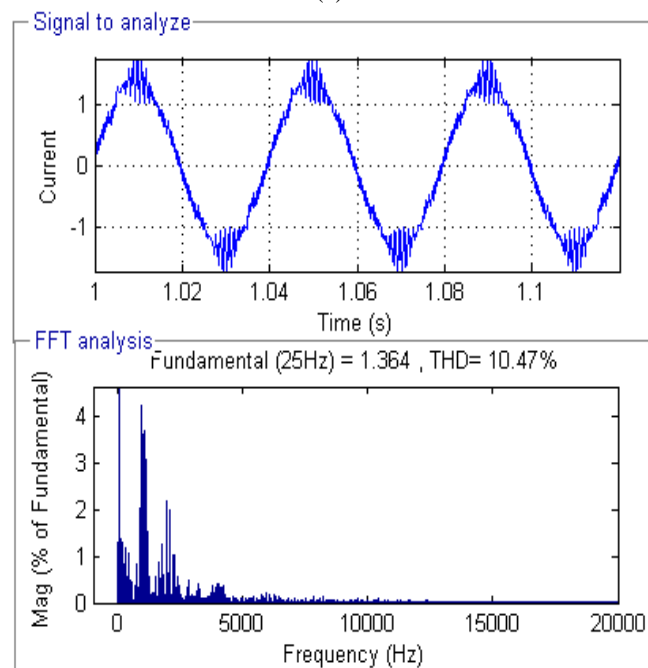

(a)

(b)

Fig.12. Output waveforms along with THD at modulation index of 0.61. a) Motor voltage b) Motor No-load current

Fig.10 shows simulation result of V/F controlled open end winding induction motor controlled by two two-level inverters at MI of 0.86. Fig.10(a), shows motor voltage waveform with THD of 15.60% and Fig.10(b) shows motor current waveforms with THD of 6.70%. Similarly Fig.11 shows simulation results along with their related THD at MI of 0.77. Fig.11(a), shows motor voltage waveform with THD of 15.74% and Fig.11(b) shows motor current waveforms with THD of 6.02%.

Fig.12 shows simulation result with their related THD at MI of 0.61. Fig.12(a), shows motor voltage waveform with THD of 25.91% and Fig.12(b) shows motor current waveforms with THD of 6.66%. Similarly, Fig.13 shows simulation results along with their related THD at MI of 0.42. Fig.13(a), shows motor voltage waveform with THD of 45.54% and Fig.13(b) shows motor current waveforms with THD of 10.47%.

(a)

(b)

Fig.13. Output waveforms along with THD at modulation index of 0.43. a) Motor voltage b) Motor No-load current

From the Fig.10 to Fig.13, it is observed that the harmonic dominance is at multiple of switching frequencies only. So that by adopting a higher switching frequency, the inverter's performance is improved.

4. Experimental Results

The implementation of proposed SVM algorithm using dSPACE1104 RTI control desk is done on volts/Hz controlled open end winding induction motor fed by IGBT based two two-level inverter. The parameters of the induction motor considered for testing are 3-Φ, 0.75kW, 415V, 1.8A, and 1415 rpm. The experimental setup was shown in Fig.14. The motor input voltage and current are captured using a Textronix TDS 2014 C series digital storage oscilloscope with sensors and results are presented in Fig.15 to Fig.18. Further simulation results are validated and compared with experimental results.
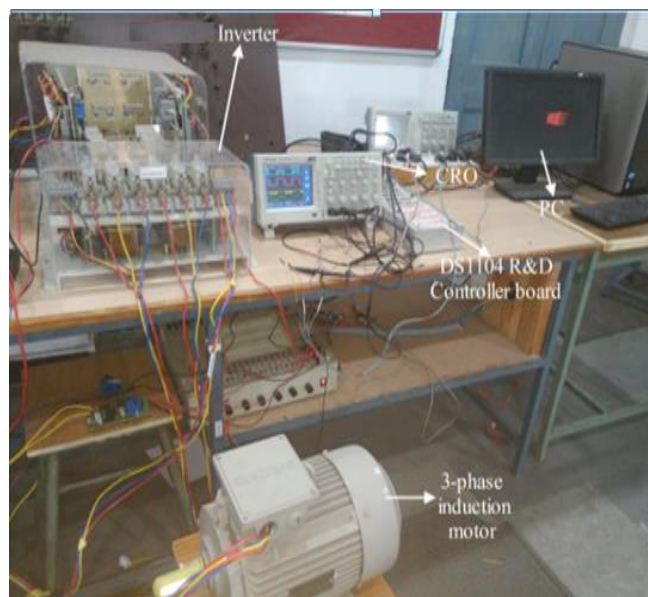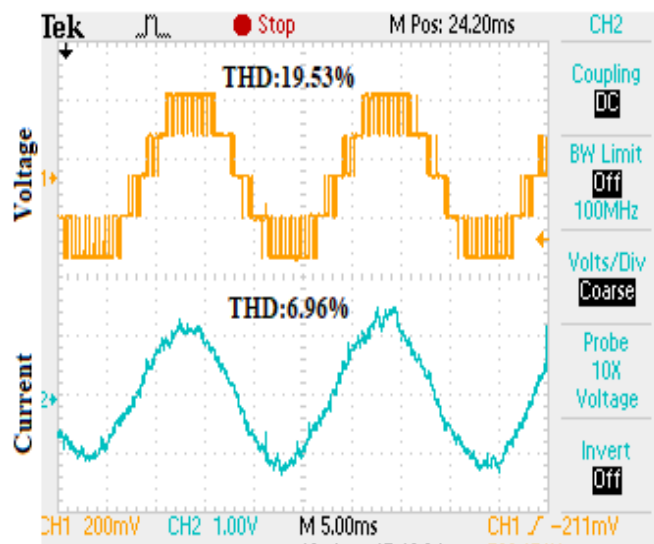

Fig.14. Experimental Setup

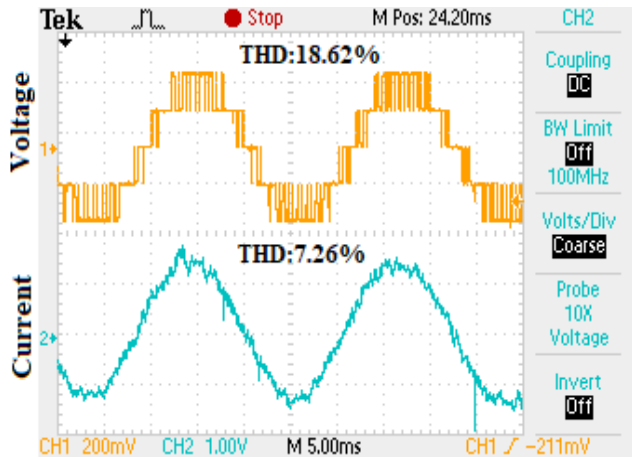**Fig.15.** Plot of Motor voltage and current at MI of 0.86

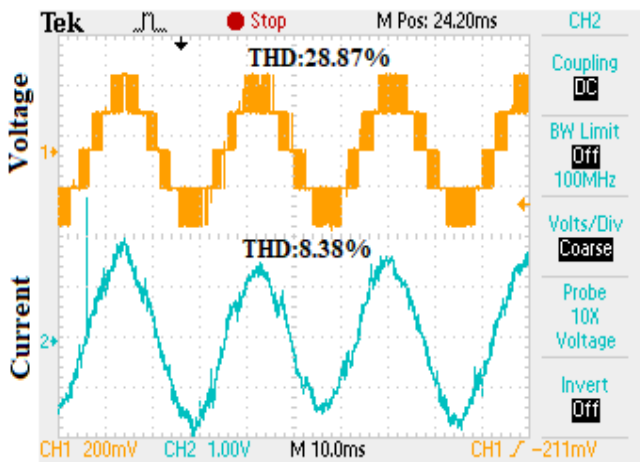**Fig.16.** Plot of Motor voltage and current at MI of 0.77

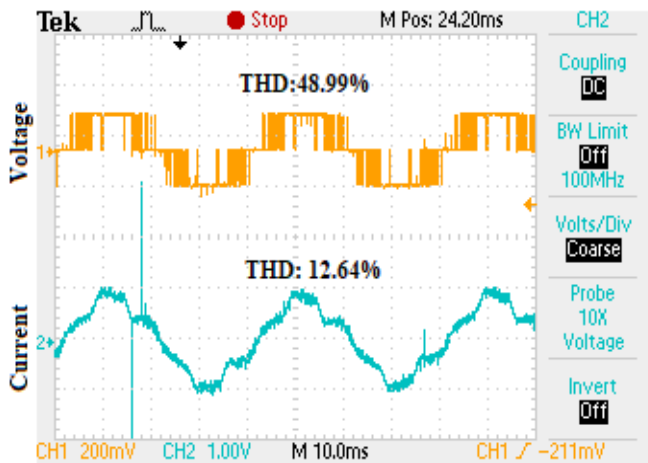**Fig.17.** Plot of Motor voltage and current at MI of 0.61

Fig. 18. Plot of Motor voltage and current at MI of 0.43

Fig.15 to Fig.18 shows motor line voltage and current waveforms along with the numerical THD values at various MI. If MI of an MLI is decreased from its peak value of 0.866, the same three level MLI produces less levels in the output. It can be observed in Fig.13 and Fig.18, they having only two levels in the output at MI of 0.43 with increased THD. Comparison of Motor voltage THD and no-load current THD for simulation and experimental results are shown in Table 5. By the values in the Table 5 it is clear that, only slight acceptable difference between simulation and experimental results.

Table 5. Motor input voltage and Current THD

MI	Current THD		Voltage THD	
	Experimental	Simulation	Experimental	Simulation
0.865	7.98	7.58	26.62	23.88
0.86	6.96	6.70	19.53	15.60
0.83	7.67	6.63	17.67	14.66
0.77	7.26	6.02	18.62	15.74
0.61	8.38	6.66	28.87	25.91
0.52	8.96	7.68	27.22	21.37
0.43	12.64	10.47	48.99	45.54
0.35	12.88	11.34	67.41	77.21

5. Conclusion

A simplified SVPWM algorithm using integer factor approach is developed and implemented on open end winding induction motor. The newly developed algorithm is initially verified through simulation using MATLAB and then implemented practically with IGBT based Inverters. The dSPACE 1104 control desk is interfaced to generate the required pulses for the inverter. The present algorithm is developed based on the space vector approach and completely implemented through digital approach. The paper focuses on the conventional switching sequence of 0127 to generate PWM pulses. In 0127 sequence the zero state duration is placed equally at both ends with in the switching cycle. The results are presented for a switching frequency of 2kHz. The proposed algorithm is generalized for any number of levels and can be easily extended to advanced discontinuous PWM sequences utilizing either or both the zero states and considering the active state division also. In future the present work can be extended to Discontinuous PWM's like DPWM MIN, DPWM MAX, DPWM ZERO, DPWM ONE, DPWM TWO and DPWM THREE for grid connected MLIs.

References

[1] Allaoui, Tayeb, and Chaker Abdelkader. "Power Quality Improvement Based on Five-Level Shunt APF Using Sliding Mode Control Scheme Connected to a Photovoltaic." International Journal of Smart Grid-ijSmartGrid, vol. 1, no. 1, pp. 9-15, 2017.

[2] V. Fernão Pires, D. M. Sousa and J. F. Martins, "Three-phase nine switch inverter for a grid-connected photovoltaic system," 2013 International Conference on Renewable Energy Research and Applications (ICRERA), pp. 1078-1083, 2013.

[3] Benbouhenni, Habib. "Application of five-level NPC inverter in DPC-ANN of doubly fed induction generator for wind power generation systems." International Journal of Smart Grid-ijSmartGrid, vol. 3, no. 3, pp. 128-137, Sep 2019.

[4] H. Abu Bakar Siddique, A. R. Lakshminarasimhan, C. I. Odeh and R. W. De Doncker, "Comparison of modular multilevel and neutral-point-clamped converters for medium-voltage grid-connected applications," 2016

IEEE International Conference on Renewable Energy Research and Applications (ICRERA), pp. 297-304, 2016.

[5] Benbouhenni, Habib. "Direct power control of a DFIG fed by a seven-level inverter using SVM strategy." International Journal of Smart Grid, vol. 3, no. 2, pp. 54-62, june 2019.

[6] S. Benanti, C. Buccella, M. Caruso, V. Castiglia, C. Cecati, A. O. Di Tommaso, R. Miceli, P. Romano, G. Schettino, F. Viola, "Experimental analysis with FPGA controller-based of MC PWM techniques for three-phase five level cascaded H-bridge for PV applications," 2016 IEEE International Conference on Renewable Energy Research and Applications (ICRERA), pp. 1173-1178, 2016. doi: 10.1109/ICRERA.2016.7884518.

[7] Rao SN, Kumar DA, Babu and CS. "Implementation of Cascaded based Reversing Voltage Multilevel Inverter using Multi Carrier Modulation Strategies." International Journal of Power Electronics and Drive Systems. Vol. 8, no.6, pp. 4047-4059, 2018.

[8] Rao SN, Ashok Kumar DV and Babu C. "Grid Connected Distributed Generation System with High Voltage Gain Cascaded DC-DC Converter Fed Asymmetric Multilevel Inverter Topology." International Journal of Electrical & Computer Engineering, Vol. 9, no.1, pp. 220-230, 2018.

[9] W. X. Yao, H. B. Hu, and Z. Y. Lu, "Comparisons of space-vector modulation and carrier-based modulation of multilevel inverter," IEEE Transactions on Power Electronics, vol. 23, No. 1, January 2008.

[10] Amit Kumar Gupta, and Ashwin M. Khambadkone, "A Space Vector PWM Scheme for Multilevel Inverters Based on Two-Level Space Vector PWM," IEEE Transactions on Industrial Electronics, vol. 53, no. 5, October 2006.

[11] Pratheesh. K, Jagadanand, Rijil Ramchand, "An Improved Space Vector PWM Method for a Three-Level Inverter with Reduced THD," 2015 9th International Conference on Compatibility and Power Electronics (CPE). IEEE, pp. 167-172, June 2015.

[12] R. Baranwal, K. Basu and N. Mohan, "Carrier-Based Implementation of SVPWM for Dual Two-Level VSI and Dual Matrix Converter With Zero Common-Mode Voltage," IEEE Transactions on Power Electronics, vol. 30, no. 3, pp. 1471-1487, March 2015.

[13] N. Jarutus and Y. Kumsuwan, "A Carrier-Based Phase-Shift Space Vector Modulation Strategy for a Nine-Switch Inverter," IEEE Transactions on Power Electronics, vol. 32, no. 5, pp. 3425-3441, May 2017.

[14] S. Das and G. Narayanan, "Novel switching sequences for a space vector modulated three level inverter," IEEE Transactions on Industrial Electronics, vol. 59, no. 3, pp. 1477-1487, Mar. 2012.

[15] K. Gupta, A. M. Khambadkone and K. M. Tan, "A space vector PWM scheme for multilevel inverters based on two level svpwm", IEEE Transactions on Industrial Electronics, vol. 53 no. 5, pp. 1631-1639, Oct. 2006.

[16] Gopinath and A. Mohamed, "Fractal based space vector PWM for multilevel inverters-A novel approach," IEEE Transactions on Industrial Electronics, vol. 56 no. 4, pp. 1230-1237, Apr. 2009.

[17] P. Chamarthi, Pawan Chhetri and Vivek Agarwal, "Simplified Implementation scheme for Space Vector Pulse Width Modulation of n-level Inverter with Online Computation of Optimal Switching Pulse Durations", IEEE Transactions on Industrial Electronics, vol. 63 no. 11, pp. 1631-1639, Nov. 2016.

[18] S. B. Bahir, A. R. Beig and M. Poshtan, "An improved space vector PWM for grid connected MMC," 2017 IEEE 6th International Conference on Renewable Energy Research and Applications (ICRERA), pp. 556-561, 2017.

[19] Xiong Li, Serkan Dusmez, Udupi Rajagopal Prasanna, Bilal Akin, and Kaushik Rajashekara, "New SVPWM Modulated Input Switched Multilevel Converter for Grid-Connected PV Energy Generation Systems" IEEE Journal Of Emerging And Selected Topics In Power Electronics, Vol. 2, No. 4, December 2014.

[20] Xiong Li, Serkan Dusmez, Bilal Akin, and Kaushik Rajashekara, "A New SVPWM for the Phase Current Reconstruction of Three-Phase Three-level T-type Converters," IEEE Transactions On Power Electronics, Vol. 31, No. 3, pp. 2627–2637, March 2016.

[21] Kumar, A. Suresh, K. Sri Gowri, and M. Vijay Kumar. "New Generalized SVPWM Algorithm for Multilevel Inverters." journal of power electronics, vol. 18, no. 4, pp. 1027-1036, July 2018.

[22] A. Suresh kumar, K. Sri Gowri, and M. Vijaya Kumar. "Decomposition-Based New Space Vector Modulation Algorithm for Three-Level Inverter with Various ADSVPWM Strategies." Journal of Circuits, Systems and Computers, vol. 29, no. 06, pp. 2050090, May 2020.

[23] A. Suresh kumar, K. Sri Gowri, and M. Vijaya Kumar. "Performance study of various discontinuous PWM strategies for multilevel inverters using generalized space vector algorithm." Journal of Power Electronics, vol. 20, no. 1, pp. 100-108, Jan 2020.

[24] Anisetty Suresh Kumar, K. Sri Gowri, Nagaraja Rao S, Manjunatha BM, Sesi Kiran P, and Niteesh Kumar K. "Integer factor based SVPWM approach for multilevel inverters with continuous and discontinuous switching sequences." Archives of Electrical Engineering. Vol. 70, no. 4, pp. 859-872, Dec 2021.